J. Fluid Mech. (1975), *vol.* 68, *part* 3, *pp.* 537–566
Printed in Great Britain

Progress in the development of a Reynolds-stress turbulence closure

By B. E. LAUNDER, G. J. REECE
AND W. RODI†

Department of Mechanical Engineering, Imperial College, London

(Received 18 February 1974)

The paper develops proposals for a model of turbulence in which the Reynolds stresses are determined from the solution of transport equations for these variables and for the turbulence energy dissipation rate ϵ. Particular attention is given to the approximation of the pressure–strain correlations; the forms adopted appear to give reasonably satisfactory partitioning of the stresses both near walls and in free shear flows.

Numerical solutions of the model equations are presented for a selection of strained homogeneous shear flows and for two-dimensional inhomogeneous shear flows including the jet, the wake, the mixing layer and plane channel flow. In addition, it is shown that the closure does predict a very strong influence of secondary strain terms for flow over curved surfaces.

1. Introduction

Recently a number of efficient numerical procedures have been published for solving the equations governing three-dimensional fluid flow (e.g. Patankar & Spalding 1972). This development emphasizes the need for models of turbulence more generally applicable than those based on the notion of effective turbulent transport coefficients. For, while 'effective viscosity' models have led to satisfactory predictions of many two-dimensional thin shear flows, their use in three-dimensional flows and other flows with more than a single significant component of mean velocity gradient has achieved, at best, only moderate success. One may cite turbulence-driven secondary flows in non-circular ducts or the influence of swirl on jet spreading rates as examples of phenomena which cannot satisfactorily be predicted with models of the effective-viscosity type.

There is a widely held view (Donaldson 1971; Hanjalić & Launder 1972*b*; Bradshaw 1972) that the most promising class of turbulence models for making numerical calculations of such complex flows is that based on the solution of approximated equations for the Reynolds stresses $-\overline{u_i u_j}$. A model of this kind was first proposed by Rotta (1951) and a few predictions have recently been obtained with closures of the same type by Daly & Harlow (1970), Reynolds (1970), Donaldson (1971), Naot, Shavit & Wolfshtein (1972) and Lumley & Khajeh-Nouri (1974).

The range of flows considered in each of these papers was clearly too narrow to

† Present address: Sonderforschungsbereich 80, University of Karlsruhe, Germany.

permit conclusions to be drawn regarding the range of applicability of the models presented. The approximated Reynolds-stress equations attempt to provide simulations of the dissipative, diffusive and redistributive processes appearing in the exact equations for the $\overline{u_i u_j}$. If attention is limited to just one or two types of flow, one may be led to conclude that one is imitating these processes correctly; however, a wider inquiry embracing flows where the relative magnitudes of the processes are very different may show large discrepancies between predicted and measured behaviour.

An extensive set of predictions of thin shear flows was presented by Hanjalić & Launder (1972*b*, hereafter designated HL). But, although HL developed a general Reynolds-stress closure, when it came to *solving* the equations, their model was simplified to one where the shear stress and the *sum* of the normal stresses were the only Reynolds-stress elements found. This simplified model, though adequate for the flows examined by its originators, is not suitable for the more general three-dimensional flows mentioned above. Our purpose here, therefore, is to present the outcome of predicting a similar range of turbulent flows, only now employing a *complete* Reynolds-stress closure. The flows examined include a number of free shear flows (jet, wake and mixing layer), plane channel flow (both symmetric and asymmetric) and three cases of distorted homogeneous turbulence.

Sections 2 and 3 below develop the form (or rather forms) of the stress closure we have examined; the applicability of the model is limited to regions of flow where the turbulent Reynolds number is large. Most attention has been given to the approximation of the correlations between pressure and strain fluctuations, which play such a dominant role in the evolution of the flow. Although HL made proposals for approximating these terms, the extra constraints imposed by the need (in the present work) to account not just for the shear stress but for the three normal stresses too have forced a reappraisal; this appears as § 2. Closure is completed in § 3, where we adopt previously proposed approximations for the remaining unknown quantities in the $\overline{u_i u_j}$ and ϵ equations.

Section 4 compares the calculated and measured behaviour of the test cases, beginning with three homogeneous flows and proceeding to the two-dimensional shear flows. Finally § 5 discusses what seem to be the best routes for improving the model in its present form.

2. Approximation of the pressure–strain correlations

2.1. *Turbulence remote from walls*

The set of differential equations governing the transport of the (kinematic) Reynolds stresses $-\overline{u_i u_j}$ may be written in the form

$$\frac{D\overline{u_i u_j}}{Dt} = \underbrace{-\left[\overline{u_j u_k}\frac{\partial U_i}{\partial x_k} + \overline{u_i u_k}\frac{\partial U_j}{\partial x_k}\right]}_{\text{generation}} \underbrace{- 2\nu\overline{\frac{\partial u_i}{\partial x_k}\frac{\partial u_j}{\partial x_k}}}_{\text{dissipation}} \underbrace{+ \overline{\frac{p}{\rho}\left(\frac{\partial u_i}{\partial x_j} + \frac{\partial u_j}{\partial x_i}\right)}}_{\substack{\text{pressure} \\ \text{strain}}}$$

$$\underbrace{- \frac{\partial}{\partial x_k}\left[\overline{u_i u_j u_k} - \nu\frac{\partial \overline{u_i u_j}}{\partial x_k} + \overline{\frac{p}{\rho}(\delta_{jk}u_i + \delta_{ik}u_j)}\right]}_{\text{diffusion}}, \qquad (1)$$

where upper and lower case u's denote mean and fluctuating components of velocity, p is the fluctuation of static pressure about its mean value and x's denote Cartesian space co-ordinates.

To convert (1), the mean-motion equations and the continuity equation into a closed set of equations for mean velocities and Reynolds stresses, the turbulence quantities on the right-hand side of (1) must be represented as empirical functions of the mean velocities and Reynolds stresses and their derivatives. In this section we consider the approximation of the pressure–strain correlation, the third group of terms on the right side of (1). Following Chou (1945), the explicit appearance of the pressure in the correlation is eliminated by taking the divergence of the equation for the fluctuating velocity u_i, thus obtaining a Poisson equation for p. The pressure–strain correlation may then be re-expressed in the following form for a position $\mathbf{x}$ in the flow:

$$\overline{\frac{p}{\rho}\frac{\partial u_i}{\partial x_j}} = \frac{1}{4\pi}\int_{\text{vol}} \left\{ \underbrace{\left(\overline{\frac{\partial^2 u_l u_m}{\partial x_l \partial x_m}}\right)' \overline{\frac{\partial u_i}{\partial x_j}}}_{\phi_{ij,1}} + 2\underbrace{\left(\frac{\partial U_l}{\partial x_m}\right)' \left(\overline{\frac{\partial u_m}{\partial x_l}}\right)' \left(\overline{\frac{\partial u_i}{\partial x_j}}\right)}_{\phi_{ij,2}} \right\} \frac{d\,\text{vol}}{|\mathbf{x}-\mathbf{y}|} + S_{ij}, \qquad (2)$$

where terms with and without a prime relate to values at $\mathbf{y}$ and $\mathbf{x}$ respectively (the integration being carried out over $\mathbf{y}$ space), and S_{ij} is a surface integral which will be negligible away from the vicinity of a solid boundary. Equation (2) suggests that there are two distinct kinds of interaction giving rise to the correlation $\overline{p\,\partial u_i/\partial x_j}$; one involving just fluctuating quantities ($\phi_{ij,1}$) and another arising from the presence of the mean rate of strain ($\phi_{ij,2}$).

Nearly every worker who has made closure approximations for (1) has adopted Rotta's (1951) proposal for $\phi_{ij,1}$, which may be written as

$$\phi_{ij,1} + \phi_{ji,1} = -c_1(\epsilon/k)\,(\overline{u_i u_j} - \tfrac{2}{3}\delta_{ij}k), \qquad (3)\dagger$$

where c_1 is supposed to be a constant (at any rate, at high Reynolds numbers) and k and ϵ are the time-averaged turbulence kinetic energy and energy dissipation rate respectively: the quotient k/ϵ thus represents a characteristic decay time of the turbulence. According to (3), the sign of $\phi_{ij,1}$ is always such as to promote a change towards isotropy, its magnitude being proportional to the local level of anisotropy. Rotta (1951) originally proposed that c_1 should be about 1·4, though later (Rotta 1962) he showed that a value about twice as large provided a better fit to Uberoi's (1957) data on the decay of highly anisotropic turbulence. We do not, however, regard the data as entirely conclusive. For these and the later measurements of Tucker & Reynolds (1968) the turbulence Reynolds number is rather low. It is probable therefore that in both experiments the dissipative motions were not isotropic, thus indicating a spuriously high value of c_1. In the present work we have explored the proposition that the apparent variation of c_1 from one flow to another could be correlated in terms of the local degree of anisotropy of the turbulence. Eventually it was concluded, however, that there was no overall advantage to be gained in this way. For the solutions presented in § 4, therefore, c_1 takes a constant value.

Some of the proposals for closing the Reynolds-stress equation have assumed that $\phi_{ij,1}$ is the only significant contributor to $\overline{p\,\partial u_i/\partial x_j}$ (Donaldson 1968, 1971;

† Hereafter, for brevity, $\phi_{ij,1} + \phi_{ji,1}$ is denoted by $\phi_{ij,1}$.

Lumley 1972; Daly & Harlow 1970).† This conclusion appears supportable provided that one makes predictions over only a narrow range of turbulent shear flows; for then the effects of omitting $\phi_{ij,2}$ can be absorbed either through the value ascribed to c_1 or through the way the decay terms in (1) are simulated. Reynolds (1970) has shown, however, that prediction of a range of even homogeneous free turbulent flows demands the inclusion of mean strain rates in the pressure–strain terms. Moreover, both Crow (1968) and Townsend (1954) have shown that under conditions of rapid distortion the effect of $\phi_{ij,2}$ far outweighs that of $\phi_{ij,1}$.

Our practice in simulating $\phi_{ij,2}$ also takes its direction from Rotta's (1951) paper. We assume that this correlation may be approximated in the form

$$\phi_{ij,2} = (\partial U_l/\partial x_m)\, a_{lj}^{mi}, \tag{4}$$

where

$$a_{lj}^{mi} = -\frac{1}{2\pi}\int_{\text{vol}} \frac{\partial^2 \overline{u'_m u_i}}{\partial \xi_l \partial \xi_j}\frac{d\,\text{vol}}{|\mathbf{x}-\mathbf{y}|}$$

and the ξ's are the Cartesian components of the position vector $\mathbf{x}-\mathbf{y}$. Equation (4) is a rigorous consequence of (2) when all second derivatives of the mean velocity are negligible and the turbulence field may be taken as homogeneous; it is of course only approximately true in more general flows. Rotta (1951) has commented that the fourth-order tensor $\{a_{lj}^{mi}\}$ should satisfy the following kinematic constraints:

$$a_{lj}^{mi} = a_{lj}^{im} = a_{jl}^{im}, \tag{5}$$

$$a_{li}^{mi} = 0, \quad a_{jj}^{mi} = 2\overline{u_m u_i}. \tag{6), (7}$$

The form of (7) suggests that a_{lj}^{mi} might be satisfactorily approximated by a linear combination of Reynolds stresses. The most general such tensor satisfying the symmetry constraints implied by (5) may be written as

$$\begin{aligned} a_{lj}^{mi} = {} & \alpha\delta_{lj}\overline{u_m u_i} + \beta(\delta_{ml}\overline{u_i u_j} + \delta_{mj}\overline{u_i u_l} + \delta_{il}\overline{u_m u_j} + \delta_{ij}\overline{u_m u_l}) \\ & + c_2\delta_{mi}\overline{u_l u_j} + [\eta\delta_{mi}\delta_{lj} + \upsilon(\delta_{ml}\delta_{ij} + \delta_{mj}\delta_{il})]k, \end{aligned} \tag{8}$$

where α, β, c_2, η and υ are constants. The application of (6) and (7) enables four of these constants to be expressed in terms of the fifth: in terms of c_2

$$\begin{aligned} \alpha &= \tfrac{1}{11}(4c_2+10), & \beta &= -\tfrac{1}{11}(2+3c_2), \\ \eta &= -\tfrac{1}{55}(50c_2+4), & \upsilon &= \tfrac{1}{55}(20c_2+6). \end{aligned} \tag{9}$$

Equations (8) and (9) were in fact developed during the HL work but eventually were not adopted there because with c_1 assigned a value of about 2·8 (i.e. the value that Uberoi's (1957) data seemed to imply) they led to much too small differences between the normal stresses in the nearly homogeneous shear flow of Champagne, Harris & Corrsin (1970). As remarked above, however, we now feel less certain about the best value for c_1. On balance, it seemed preferable to adopt the form of $\phi_{ij,2}$ expressed by (4), (8) and (9) and to let c_1 take on a suitably

† In the Daly–Harlow work the influence of mean strain rates does enter indirectly, however, because the magnitude of c_1 depends on the ratio of the generation to the dissipation rates of turbulence energy.

smaller value, rather than to retain the published HL form, which failed to satisfy (7) in all respects and which was therefore expected to give specious effects in complex strain fields.

On combining (4), (8) and (9) the complete influence of the mean strain on the pressure–strain correlation may be expressed in the following compact form:

$$(\phi_{ij}+\phi_{ji})_2 = -\frac{(c_2+8)}{11}\{P_{ij}-\tfrac{2}{3}P\delta_{ij}\}-\frac{(30c_2-2)}{55}k\left\{\frac{\partial U_i}{\partial x_j}+\frac{\partial U_j}{\partial x_i}\right\} -\frac{(8c_2-2)}{11}\{D_{ij}-\tfrac{2}{3}P\delta_{ij}\}, \quad (10)$$

where $$P_{ij} \equiv -\left\{\overline{u_i u_k}\frac{\partial U_j}{\partial x_k}+\overline{u_j u_k}\frac{\partial U_i}{\partial x_k}\right\}, \quad D_{ij} \equiv -\left\{\overline{u_i u_k}\frac{\partial U_k}{\partial x_j}+\overline{u_j u_k}\frac{\partial U_k}{\partial x_i}\right\}$$

and P denotes the rate of production of turbulence energy.

Perhaps the first point to note is that (10) is equivalent to a recent proposal of Naot, Shavit & Wolfshtein (1973).† These authors pursued a considerably more elaborate analysis than the present one in which a shape was assumed for the two-point correlation function $\overline{u_i u_j'}$, thus enabling the integrand in (4) to be evaluated. The fact that (10) has been reached merely from kinematic arguments indicates that some of the postulates in Naot's work were redundant. It is interesting to note also that for the case of isotropic turbulence subjected to sudden distortion, irrespective of the value of c_2, equation (10) reduces to

$$(\phi_{ij}+\phi_{ji})_2 = 0{\cdot}4k(\partial U_i/\partial x_j+\partial U_j/\partial x_i), \quad (11)$$

which is the exact result derived by Crow (1968), again by way of a more elaborate analysis.

We have also tried a degenerate form of (10). Since each of the three groups of terms on the right side of (11) vanishes under contraction of indices, one may discard either one or two of the groups without removing the essential property that the term as a whole should be redistributive in character.‡ The first group on the right side of (10) turns out to be the dominant one and, because of its clear physical significance, it is interesting to discover to what extent this term alone can account for the mean-strain effects in the pressure–strain correlation, i.e.

$$(\phi_{ij}+\phi_{ji})_2 = -\gamma(P_{ij}-\tfrac{2}{3}P\delta_{ij}). \quad (12)$$

It is to be expected that the constant γ will differ somewhat in magnitude from the coefficient of the first term in (10) to compensate in part for the neglected terms. Note that for isotropic turbulence (11) is satisfied if γ takes the value 0·6; so if (12) is to be a useful approximation in more general flows the 'best' value of γ should be near this value. Equation (12) is the counterpart of Rotta's proposal for $\phi_{ij,1}$: as Rotta's term acts to diminish the anisotropy of the stress field so, according to (12), $(\phi_{ij}+\phi_{ji})_2$ tends to isotropize the turbulence production tensor. Equation (12) has already been proposed by Naot, Shavit &

† The appearance of Naot's proposal is a little different from (10) owing to the different analytical paths followed.

‡ Equation (5) however is not satisfied.

Wolfshtein (1970) as a *replacement* for $\phi_{ij,1}$. In our work we have used it in addition to Rotta's tendency-to-isotropy term.

An empirical constant appears in both the 'complete' and the simplified approximations to the second part of the pressure–strain term. The most direct information about these constants is given by the nearly homogeneous shear flow of Champagne *et al.* (1970), where U_1 varies linearly with x_2. In this flow diffusive stress transport is insignificant throughout and convective influences are small at the downstream end of the test section. Thus, if we neglect the transport terms from (1), incorporate the pressure–strain approximations discussed above and (as proposed in § 3) assume the dissipative motions to be isotropic, (1) reduces to a set of algebraic formulae for the normal stresses. For the more elaborate pressure–strain model there results

$$\left.\begin{aligned}(\overline{u_1^2}-\tfrac{2}{3}k)/k &= (8+12c_2)/33c_1 \quad (\simeq 0{\cdot}3),\\ (\overline{u_2^2}-\tfrac{2}{3}k)/k &= (2-30c_2)/33c_1 \quad (\simeq -0{\cdot}18),\\ (\overline{u_3^2}-\tfrac{2}{3}k)/k &= (-10+18c_2)/33c_1 \quad (\simeq -0{\cdot}12).\end{aligned}\right\} \tag{13}$$

The experimental values given in parentheses are well represented by the model formulae with c_2 approximately 0·4, provided that c_1 takes a value of about 1·5; the value of about 2·5 used by HL and others makes the normal stresses too nearly equal. The corresponding formulae for the simplified model [equation (12)] are

$$\left.\begin{aligned}(\overline{u_1^2}-\tfrac{2}{3}k)/k &= 4(1-\gamma)/3c_1,\\ (\overline{u_2^2}-\tfrac{2}{3}k)/k &= -2(1-\gamma)/3c_1,\\ (\overline{u_3^2}-\tfrac{2}{3}k)/k &= -2(1-\gamma)/3c_1.\end{aligned}\right\} \tag{14}$$

Because there is no direct production of $\overline{u_2^2}$ or $\overline{u_3^2}$ these normal stresses are equal in magnitude when the simpler pressure–strain hypothesis is used; thus it cannot match the experimental result that the lateral stress component is somewhat larger than the transverse one. However, these differences are not so large as to disqualify (12) from further consideration.† With γ set to equal 0·6 to satisfy (11), the experimental values are again tolerably well matched with c_1 about 1·5.

2.2. *Near-wall turbulence*

Let us compare the relative stress levels in near-wall turbulence with those in the homogeneous shear layer mentioned above. Both are flows where convection and diffusion of the Reynolds stresses are small and where, in consequence, turbulence energy generation and dissipation rates are very nearly in balance. The approximations made so far for the pressure–strain correlation imply that the relative magnitudes of the Reynolds stresses will be the same in each of these flows. Table 1, which summarizes experimental data, shows, however, that near a wall the streamwise stress component is appreciably larger and the transverse component much smaller than in the homogeneous free shear layer. The level of $\overline{u_1u_2}/k$ is also appreciably smaller in the near-wall flow.

† The larger differences between $\overline{u_2^2}$ and $\overline{u_3^2}$ found in near-wall turbulence are due to the wall proximity, as discussed in § 2.2.

	$\overline{u_1^2}/k-\frac{2}{3}$	$\overline{u_2^2}/k-\frac{2}{3}$	$\overline{u_3^2}/k-\frac{2}{3}$	$-\overline{u_1u_2}/k$
Plane homogeneous shear layer (Champagne *et al.* 1970)	0·30	−0·18	−0·12	0·33
Near-wall turbulence (a consensus of near-wall turbulence data)	0·51	−0·42	−0·09	0·24

TABLE 1. Reynolds stresses in equilibrium shear flows

These results suggested that (4) did not adequately approximate the influences of mean strain on the pressure–strain term when the mean velocity gradient varied rapidly in space. Accordingly, following Rotta (1951) we generalized (4) to

$$\phi_{ij,2} = a_{lj}^{mi}\frac{\partial U_l}{\partial x_m} + {}_{nk}c_{lj}^{mi}\frac{\partial^3 U_l}{\partial x_n\,\partial x_k\,\partial x_m}, \tag{15}$$

where

$${}_{nk}c_{lj}^{mi} = -\frac{1}{4\pi}\int_{\text{vol}}\frac{\partial^2\overline{u_m u_i}}{\partial\xi_l\,\partial\xi_j}\xi_n\xi_k\frac{d\,\text{vol}}{|\mathbf{x}-\mathbf{y}|}. \tag{16}$$

This form has been extensively tested, the quantity ${}_{nk}c_{lj}^{mi}$ being approximated by methods parallel to those adopted for choosing a_{lj}^{mi}. Nevertheless, entirely satisfactory behaviour could not be achieved, especially in the asymmetric channel flow of Hanjalić & Launder (1972*a*). As figure 1 shows, the measured normal stresses in this flow are by no means equal even in the neighbourhood of the velocity maximum. The behaviour seemed almost certainly due to a 'wall proximity' effect in the pressure–strain term; and yet $\partial^3 U_1/\partial x_2^3$ was entirely negligible in the vicinity of the maximum velocity. It was concluded, therefore,

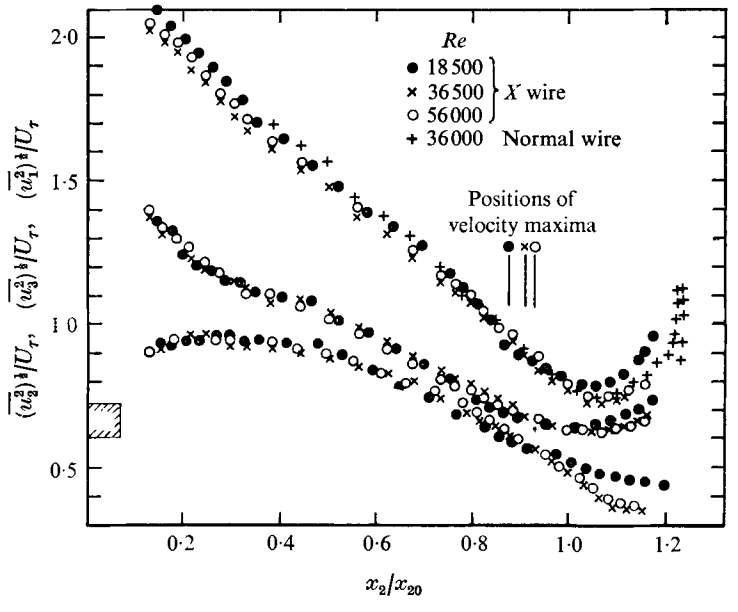

FIGURE 1. Turbulence intensity profiles in asymmetric channel flow, Hanjalić & Launder (1972*a*).

that the near-wall influence could not be attributed simply to the more rapid variation of $\partial U_l/\partial x_m$ provoked by the wall.

In fact, the conclusion reached above was hastened by Bradshaw's (1973*b*) demonstration that the *surface integral* S_{ij} in (2) would make a significant contribution to the pressure–strain correlation as long as the typical size of the energy-containing motions was of the same order as the distance from the wall. As he remarked, this condition is always satisfied in boundary layers developing on walls. In this connexion, we are grateful to Dr H. P. A. Irwin for pointing out that for a plane wall (with x_2 normal to the surface) (2) may be recast to advantage in the following form, from which the surface integral is eliminated:

$$\overline{\frac{p}{\rho}\frac{\partial u_i}{\partial x_j}} = \frac{1}{4\pi}\int_{\text{vol}} \left\{ \left(\overline{\frac{\partial^2 u_l \partial u_m}{\partial x_l \partial x_m}}\right)' \left(\overline{\frac{\partial u_i}{\partial x_j}}\right) + 2\left(\frac{\partial U_1}{\partial x_2}\right)' \left(\overline{\frac{\partial u_2}{\partial x_1}}\right)' \overline{\frac{\partial u_i}{\partial x_j}} \right\} \left[\frac{1}{|\mathbf{x}-\mathbf{y}|} + \frac{1}{|\mathbf{x}-\mathbf{y}^*|}\right] d\,\text{vol}, \tag{17}$$

where $\mathbf{y}^*$ is the image of the point $\mathbf{y}$ (i.e. its components are y_1, $-y_2$ and y_3) and the volume of integration is the region $x_2 > 0$. This form immediately suggested that there should be *two* contributions to the near-wall effect, corresponding to the reflected-wall influence of $\phi_{ij,1}$ and $\phi_{ij,2}$. Once this inference has been drawn it is easy to find support from experiments. As table 1 has shown, the wall effect increases the anisotropy of the normal stresses but tends to diminish the shear stress. Additionally, figure 1 suggests that the wall influence is felt in regions where mean strain rates are negligible. Now, a term similar to $\phi_{ij,2}$ is required to give the first of these effects while one needs an approximation like $\phi_{ij,1}$ (which is finite even when the mean strain rates are zero) to bring about the latter. Accordingly the general form of the wall-proximity effect on the pressure–strain term is taken as

$$[\phi_{ij}+\phi_{ji}]_w = \left\{ c_1' \frac{\epsilon}{k}\left(\overline{u_i u_j} - \tfrac{2}{3}\delta_{ij}k\right) + \frac{\partial U_l}{\partial x_m}\left(b_{lj}^{mi} + b_{li}^{mj}\right) \right\} f\left(\frac{l}{x_2}\right), \tag{18}$$

where l denotes the length scale of the energy-containing eddies; like $\{a_{lj}^{mi}\}$, the quantity $\{b_{lj}^{mi}\}$ is a symmetric tensor composed of linear combinations of the Reynolds stresses:

$$\begin{aligned} b_{lj}^{mi} = {} & \alpha'\delta_{lj}\overline{u_m u_i} + \beta'(\delta_{ml}\overline{u_i u_j} + \delta_{mj}\overline{u_i u_l} + \delta_{il}\overline{u_m u_j} + \delta_{ij}\overline{u_m u_l}) \\ & + c_2'\delta_{mi}\overline{u_l u_j} + [\eta'\delta_{mi}\delta_{lj} + \nu'(\delta_{ml}\delta_{ij} + \delta_{mj}\delta_{il})]k. \end{aligned} \tag{19}$$

The coefficients of b_{lj}^{mi} must satisfy $b_{li}^{mi} = 0$ in order that $\phi_{ij,w}$ be redistributive. Application of this constraint leads to

$$\alpha' + 5\beta' + c_2' = 0, \quad 2\beta' + 4\nu' + \eta' = 0. \tag{20}$$

Observing from table 1 that the value of $\overline{u_3^2}$ is, within experimental uncertainty, unaffected by the presence of a wall, we set the corresponding term b_{13}^{23} equal to zero.† Hence $\beta' = 0$ and, from (20), $\alpha' = -c_2'$. The mean-strain part of the near-wall effect may thus be written as

$$\frac{\partial U_l}{\partial x_m}\left(b_{lj}^{mi} + b_{li}^{mj}\right) = c_2'[P_{ij} - D_{ij}] + \zeta' k\left(\frac{\partial U_i}{\partial x_j} + \frac{\partial U_j}{\partial x_i}\right), \tag{21}$$

† The contribution of $c_1'(\epsilon/k)\,(\overline{u_3^2} - \frac{2}{3}k)$ is barely significant because $\overline{u_3^2}$ is close to $\frac{2}{3}k$.

where $\zeta' \equiv v' + \eta'$. The function $f(l/x_2)$ must of course vanish as l/x_2 approaches zero. Indeed in the present work it is assumed that f is directly proportional to l/x_2. It is convenient to choose the constant of proportionality such that the function takes the value unity in near-wall turbulence. With l interpreted as the dissipation length $k^{\frac{3}{2}}/\epsilon$, the coefficient of l/x_2 is easily shown to be $\kappa/a^{\frac{3}{2}}$, where κ is the von Kármán constant and $a = -\overline{u_1 u_2}/k$.

We now proceed to choose c_1', c_2' and ζ' from the near-wall counterpart of (13). With transport terms neglected from (1), the following algebraic equations are obtained (to keep the appearance simple the numerical value of c_2, given in table 2 below, has been inserted):

$$\left.\begin{aligned} (\overline{u_1^2} - \tfrac{2}{3}k)/k &= (0{\cdot}39 + 2c_2')/(c_1 - c_1'), \\ (\overline{u_2^2} - \tfrac{2}{3}k)/k &= -(0{\cdot}30 + 2c_2')/(c_1 - c_1'), \\ (\overline{u_3^2} - \tfrac{2}{3}k)/k &= -0{\cdot}09/(c_1 - c_1'). \end{aligned}\right\} \tag{22}$$

It may be verified that with $c_1' = 0{\cdot}5$ and $c_2' = 0{\cdot}06$ the stress levels given by (22) correspond exactly to those given in table 1. Moreover if ζ', which appears only in the shear-stress equation, is set to zero the following formula is obtained for $\overline{u_1 u_2}$:

$$\frac{-\overline{u_1 u_2}}{k} = \left((0{\cdot}24 + c_2')\frac{\overline{u_2^2}}{k} + 0{\cdot}18 - (0{\cdot}11 + c_2')\frac{\overline{u_1^2}}{k}\right)^{\frac{1}{2}} (1{\cdot}5 - c_1')^{\frac{1}{2}}. \tag{23}$$

Using (22) to eliminate the normal stresses and with the above values for c_1' and c_2', $-\overline{u_1 u_2}/k$ equals 0·24, again in agreement with table 1.

The form of the near-wall correction to the pressure–strain correlation finally adopted (with the numerical value 4·0 inserted for $\kappa/a^{\frac{3}{2}}$) is thus

$$(\phi_{ij} + \phi_{ji})_w = \left\{0{\cdot}125\frac{\epsilon}{k}(\overline{u_i u_j} - \tfrac{2}{3}k\delta_{ij}) + 0{\cdot}015(P_{ij} - D_{ij})\right\}\frac{k^{\frac{3}{2}}}{\epsilon x_2}. \tag{24}$$

When, as in a plane channel, two parallel walls affect the flow, it is assumed that their influence is simply additive. Thus, with obvious notation, the coefficient multiplying the contents of the curly brackets in (24) is replaced by

$$\frac{k^{\frac{3}{2}}}{\epsilon}\left[\frac{1}{x_2} + \frac{1}{(D - x_2)}\right].\dagger$$

3. The remaining closure approximations

The remaining unknown correlations in (1) are approximated in the same way as in HL; therefore only brief remarks are made in support of the approximated forms. There are three contributions in (1) to the diffusive transport of Reynolds

† The same principle applied to ducts with curved or irregular boundaries suggests that in general the coefficient might be written as

$$\left[\frac{1}{2\pi}\int\frac{k^{\frac{3}{2}}}{\epsilon}\frac{d\phi}{S},\right.$$

where $d\phi$ is the elemental solid angle subtended by a small patch on the surface a distance S from the point in question. The present work however offers no evidence to support or refute this generalization.

stress. Of these, only diffusion by turbulent velocity fluctuations is retained in the modelled set† and this is approximated as follows:

$$-\overline{u_i u_j u_k} = c_s \frac{k}{\epsilon}\left[\overline{u_i u_l}\frac{\partial \overline{u_j u_k}}{\partial x_l} + \overline{u_j u_l}\frac{\partial \overline{u_k u_i}}{\partial x_l} + \overline{u_k u_l}\frac{\partial \overline{u_i u_j}}{\partial x_l}\right]. \tag{25}$$

This form was obtained by severe simplification of the exact transport equation for $\overline{u_i u_j u_k}$. In a thin shear flow (where $U_1 \gg U_2$) the expressions for diffusive transport of u_2 and u_3 reduce to

$$-\overline{u_2^2 u_2} = 3c_s \frac{k}{\epsilon}\overline{u_2^2}\frac{\partial \overline{u_2^2}}{\partial x_2}, \qquad -\overline{u_3^2 u_2} = c_s \frac{k}{\epsilon}\overline{u_2^2}\frac{\partial \overline{u_3^2}}{\partial x_2}.$$

The approximation thus implies a gradient-driven stress diffusion but one where the effective diffusion coefficient is three times as large for $\overline{u_2^2}$ as for $\overline{u_3^2}$. For comparison, some predictions have also been made employing the simple gradient-diffusion hypothesis, proposed by Daly & Harlow (1970):

$$-\overline{u_i u_j u_k} = c_s' \frac{k}{\epsilon}\overline{u_k u_l}\frac{\partial \overline{u_i u_j}}{\partial x_l}. \tag{26}$$

For the two-dimensional thin shear flows considered in this work (26) implies an *isotropic* effective diffusion coefficient. One obvious defect of the equation is that, unlike the left side, the right side of (26) alters under permutation of the indices i, j and k. The constants c_s and c_s' are assigned the values 0·11 and 0·25 respectively on the basis of computer optimization.

The decay-rate terms in (1) are modelled by assuming the dissipative motions to be isotropic:

$$2\nu\overline{\left(\frac{\partial u_i}{\partial x_l}\right)\left(\frac{\partial u_j}{\partial x_l}\right)} = \tfrac{2}{3}\delta_{ij}\epsilon. \tag{27}$$

Several experimental studies have shown that turbulence does not remain locally isotropic in the presence of strong strain fields (e.g. Townsend 1954; Uberoi 1957). Nevertheless (27) seemed to be the best of the simple hypotheses.

The final approximated form of the Reynolds-stress equation may thus be written as

$$\begin{aligned}\frac{D\overline{u_i u_j}}{Dt} = &-\left[\overline{u_j u_k}\frac{\partial U_i}{\partial x_k} + \overline{u_i u_k}\frac{\partial U_j}{\partial x_k}\right] - \tfrac{2}{3}\delta_{ij}\epsilon \\ &- c_1\frac{\epsilon}{k}(\overline{u_i u_j} - \tfrac{2}{3}\delta_{ij}k) + (\phi_{ij}+\phi_{ji})_2 + (\phi_{ij}+\phi_{ji})_w \\ &+ c_s\frac{\partial}{\partial x_k}\frac{k}{\epsilon}\left[\overline{u_i u_l}\frac{\partial \overline{u_j u_k}}{\partial x_l} + \overline{u_j u_l}\frac{\partial \overline{u_k u_i}}{\partial x_l} + \overline{u_k u_l}\frac{\partial \overline{u_i u_j}}{\partial x_l}\right],\end{aligned} \tag{28}$$

where $(\phi_{ij}+\phi_{ji})_2$ is given by (10) [or (12)] and $(\phi_{ij}+\phi_{ji})_w$ is the near-wall effect, given by (24).

† Neglect of transport by molecular interactions is permissible since, for the flows considered, the Reynolds number of the energy-containing motions is large. Neglect of pressure-induced diffusion follows the practice of most other workers though there seems no direct evidence to sustain or demolish the assumption.

The turbulence energy dissipation rate remains as an unknown in (28) and its value too is found by means of an approximate transport equation for that variable. Tennekes & Lumley (1972, p. 80) have shown that in flows at high turbulence Reynolds number the exact transport equation for ϵ (i.e. for the correlation $\nu\overline{(\partial u_i/\partial x_k)^2}$) takes the form

$$\frac{D\epsilon}{Dt} = -\frac{\partial}{\partial x_k}\left[\nu u_k \overline{\left(\frac{\partial u_i}{\partial x_l}\right)^2} + \frac{\nu}{\rho}\overline{\frac{\partial p}{\partial x_i}\frac{\partial u_k}{\partial x_i}}\right] - 2\nu\,\overline{\frac{\partial u_i}{\partial x_k}\frac{\partial u_i}{\partial x_l}\frac{\partial u_k}{\partial x_l}} - 2\overline{\left[\nu\frac{\partial^2 u_i}{\partial x_k \partial x_l}\right]^2}. \tag{29}$$

The three terms on the right side of (29) introduce further unknowns into the equation set describing the Reynolds stresses. The terms are not directly accessible to measurement and therefore their approximation can be verified only indirectly by determining whether the predicted level of ϵ is consistent with, say, the measured variation of the turbulence energy through a particular shear flow. In the present work we adopt the following analogue form of (29) developed and used in HL:

$$\frac{D\epsilon}{Dt} = c_\epsilon \frac{\partial}{\partial x_k}\left(\frac{k}{\epsilon}\overline{u_k u_l}\frac{\partial \epsilon}{\partial x_l}\right) - c_{\epsilon 1}\frac{\epsilon \overline{u_i u_k}}{k}\frac{\partial U_i}{\partial x_k} - c_{\epsilon 2}\frac{\epsilon^2}{k}. \tag{30}$$

The first term on the right side of (30) approximates the corresponding term in (29) responsible for the diffusive transport of ϵ. The second and third terms on the right side of (30) collectively represent the net effect of the generation of ϵ due to vortex stretching of turbulent filaments and its destruction by viscous action.†

There have been some minor changes in the values given to the coefficients in (30) from those originally proposed. HL had taken $c_{\epsilon 2}$ equal to 2·0 to cause the energy level of grid-generated turbulence to vary inversely with distance from its origin as indicated by Batchelor & Townsend's (1948) experiments. A more extensive scrutiny of the many investigations of grid turbulence has shown, however, that most data suggest that the exponent in the decay law should be at least $-1{\cdot}1$. We have accordingly adjusted $c_{\epsilon 2}$ to 1·90 to cause this slightly faster rate of decay.

The value for $c_{\epsilon 1}$ adopted by HL is retained here while c_ϵ is fixed by reference to the limiting form of (30) for near-wall turbulence, where convective transport of ϵ is negligible. By setting the energy dissipation rate equal to the generation rate, by putting the turbulent shear stress equal to the wall value and by replacing $\partial U_1/\partial x_2$ by $U_\tau/\kappa x_2$, (30) may be reduced to

$$c_\epsilon = (c_{\epsilon 2} - c_{\epsilon 1})\, U_\tau^6/\kappa^2 \overline{u_2^2} k^2, \tag{31}$$

where U_τ denotes the friction velocity. On inserting the values of the stress ratios implied by table 1 the value of c_ϵ emerges as 0·15, compared with the originally proposed value of 0·13.

Equations (28) and (30), together with the mean momentum equation, comprise the set of equations we have employed for computing the turbulent flows reported below. In the most general circumstances the model contains 8 constants

† Rotta (1972, private communication) and Lumley & Khajeh-Nouri (1974) have pointed out that HL's argument for including the mean-strain term in (30) was faulty. However, the latter acknowledge that the form adopted appears suitable.

	Symbol	Equation of first appearance	Value	Basis for determination
Model 1	c_1	(3)	1·5	Normal-stress levels in the nearly homogeneous shear flow
	c_2	(8)	0·4	
Model 2	c_1	(3)	1·5	
	γ	(12)	0·6	Distortion of isotropic turbulence [equation (11)]
	c_1'	(18)	0·5	Near-wall normal-stress levels
	c_2'	(19)	0·06	
	c_s	(25)	0·11	Computer optimization
	c_s'	(26)	0·25	
	$c_{\epsilon 1}$	(30)	1·44	Computer optimization
	$c_{\epsilon 2}$	(30)	1·90	Decay of grid turbulence
	c_ϵ	(30)	0·15	Consistency with a value of κ of about 0·41

TABLE 2. Values of the coefficients and basis for their choice

to be selected by reference to experiment. The values assigned to most of them have been mentioned above but for completeness they are all set out in table 2.

During the present study several hundred sets of predictions have been made of the test flows in which a range of different values for the coefficients have been explored and successively refined. In most cases the values given to the constants were chosen having especial regard for some feature of a particular turbulent flow with which the model should comply; the features in question are listed in the right-hand column of table 2. For two of the constants, however, we had no such predetermined target so we tried a wider range of values than for the other coefficients; in table 2 these are denoted as being chosen by 'computer optimization'. 'Model 1' refers to the full pressure–strain approximation (10); 'Model 2' denotes the simplified version (12). Numerical solutions for both models are presented for all the test cases.

4. Comparison of predictions with experiment

Comparison is made first with three homogeneous flows subjected to mean-strain distortion. For these flows, turbulence properties are uniform at any station in the flow, and (28) and (30) reduce to a system of first-order ordinary differential equations, which have been solved by Runge–Kutta integration using experimental initial values for $\overline{u_i u_j}$ and ϵ and the distribution of mean velocity along the test section. In fact the initial value of the dissipation rate was deduced as the closing term in a turbulence energy balance. Figure 2 shows predictions for the nearly homogeneous shear layer; the asymptotic values of the relative stress levels have been discussed earlier in § 2. Both models 1 and 2 underpredict the level of turbulence energy by about 6 % by the downstream end of the test section, mainly through discrepancies in predicting $\overline{u_1^2}$. Model 1 predicts the levels of $\overline{u_2^2}$ and $\overline{u_3^2}$ very closely throughout; only slight credit may be claimed

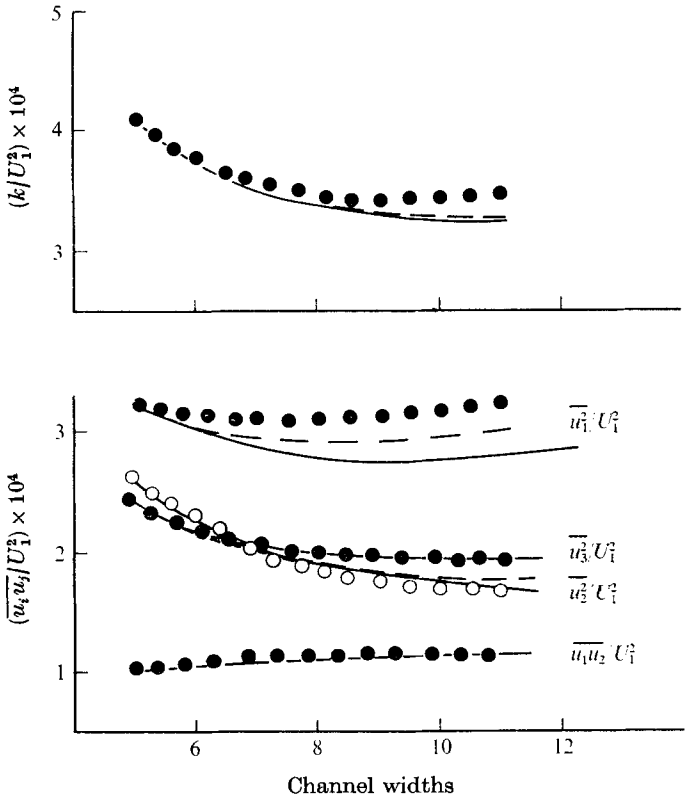

FIGURE 2. Variation of kinetic energy and Reynolds stress under nearly homogeneous shear. ○, ●, experimental data of Champagne *et al.* (1970); ——, model 1; – – – –, model 2.

however since as noted in table 2 this flow was particularly influential in choosing c_1 and c_2. Model 2, which causes a symmetric stress redistribution, gives precisely the same level for $\overline{u_2^2}$ and $\overline{u_3^2}$. Both versions accurately predict the shear-stress level in the flow.

Next we consider the plane-strain experiments of Tucker & Reynolds (1968) (see also Tucker 1970), where grid-generated turbulence passed through a rectangular duct of varying cross-section. The ratio of the sides of the duct changed from 6 : 1 to 1 : 6 with the cross-sectional area remaining constant. This was followed by a section of uniform cross-section where the relaxation of the turbulence was studied. In the computations the effects of small variations in streamwise velocity have been included although these have only a small influence on the predicted stress levels. As figure 3 indicates, the distortion greatly slows down the rate of diminution of turbulence energy; indeed, for $x_1 > 70$ in., the turbulence energy level increases. In the distorting part of the test section, figures 4 (*a*) and (*b*) (which contain results for different grids) show that the stresses are made strongly anisotropic by the distortion, more than half the kinetic energy being contained in the x_3-direction fluctuation. Model 1 leads to predicted variations very similar to those measured. Less satisfactory behaviour is obtained with the

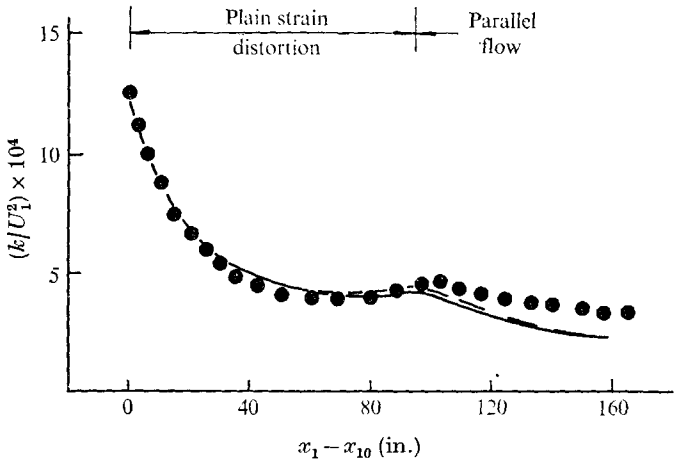

FIGURE 3. Kinetic energy variation in plane-strain distortion. ●, mean line through data of Tucker & Reynolds (1968), grid B; ——, model 1; – – –, model 2.

simpler version, model 2, the streamwise component of energy falling substantially too fast while $\overline{u_3^2}/k$ becomes too large by the end of the distortion. Also shown in figure 3 are the normal-stress levels predicted by Tucker & Reynolds using rapid-distortion theory (see Batchelor & Proudman 1954). These achieve less satisfactory agreement than either of the differential stress closures, the $\overline{u_2^2}$ component becoming far too small and the corresponding streamwise component too large.

It will be noticed that the experimental data for the two grids do not exhibit quite the same behaviour, those for grid A displaying a greater spread between $\overline{u_3^2}$ and $\overline{u_2^2}$ than those for grid C. There is even greater variation in the relaxation portion of the test section. With grid A, the components $\overline{u_3^2}$ and $\overline{u_2^2}$ revert rather quickly towards isotropy when the strain is removed; with grid C there is a much slower rise of $\overline{u_2^2}$ and scarcely any variation of $\overline{u_3^2}/k$. The predicted rates of return to isotropy lie between the extremes of the measured behaviour for the two different grids. Models 1 and 2 reduce to essentially the same form in this part of the duct because mean-strain effects are not significant; differences in the predicted values are thus due to the differences between the stress levels at the end of the distorting section.

The last homogeneous flow considered is Uberoi's (1956) 16 : 1 axisymmetric contraction experiment. Figure 5 shows that the transverse stress $\overline{u_2^2}$ is greatly enlarged by the acceleration and that the streamwise stress component also rises over the latter part of the acceleration owing to appreciable energy transfer from the u_2 and u_3 components. The predictions reproduce the trend of the measured behaviour but underpredict the magnitude of the rise in $\overline{u_2^2}$, especially model 2. The reason for the rather poor prediction of u_2 seems to be that the models for $\phi_{ij,2}$ cause too large an energy transfer from u_2 to u_1 in the initial part of the acceleration where the turbulence is nearly isotropic. Now the production rate of $\overline{u_2^2}$ is $\overline{u_2^2}\,\partial U_1/\partial x_1$; consequently too low a value of $\overline{u_2^2}$ early in the acceleration gives

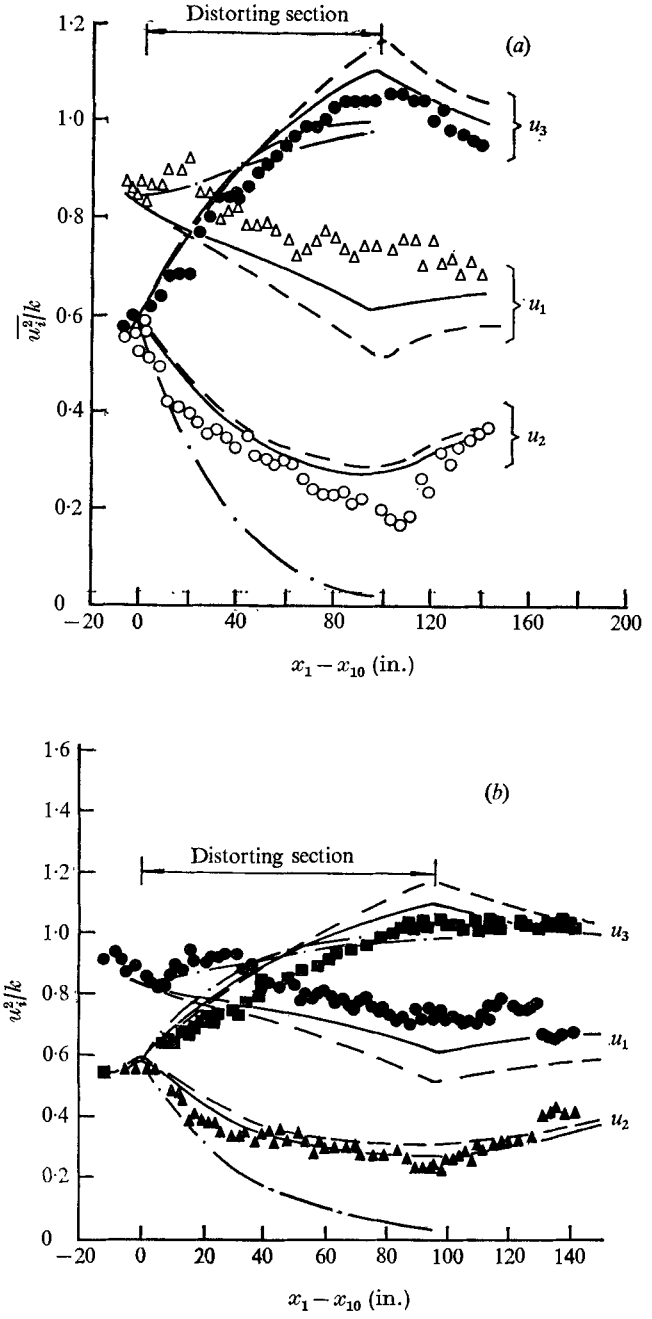

FIGURE 4. Relative normal-stress levels in plane-strain distortion (symbols denote data of Tucker 1970). (*a*) Grid *A*, Re_M = 6780. (*b*) Grid *C*, Re_M = 11700. ——, model 1; – – –, model 2; — · —, rapid-distortion theory.

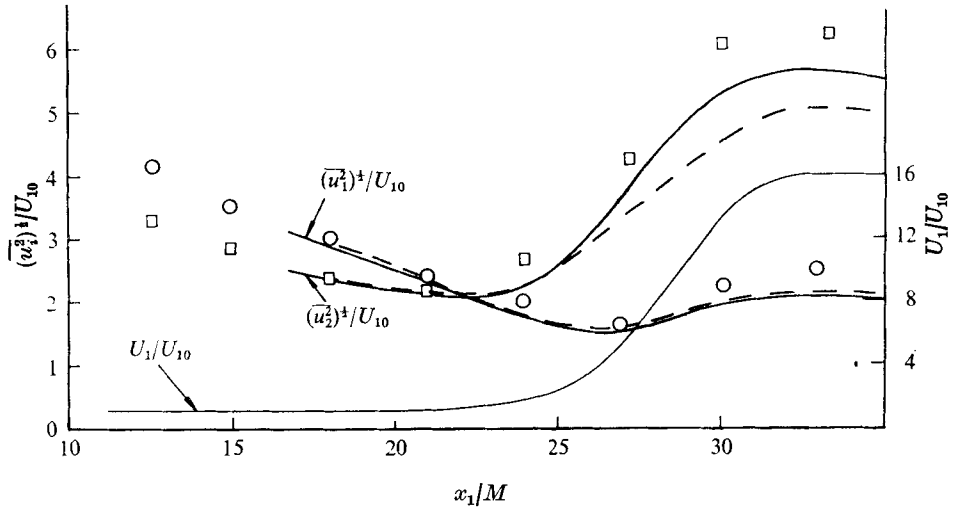

FIGURE 5. Normal-stress levels in flow through axisymmetric 16:1 contraction (symbo s denote experimental data of Uberoi 1956), model 1; – – –, model 2.

too low a generation rate of that stress component, which in turn prevents $\overline{u_2^2}$ from rising as quickly as the experiment indicates; and towards the end of the acceleration this causes too small a rate of transfer to $\overline{u_1^2}$. It is this interconnected sequence of events which causes both $\overline{u_1^2}$ and $\overline{u_2^2}$ to be 10–15 % lower than the experimental data over much of the acceleration. Calculations for Uberoi's experiment with a 9 : 1 contraction (not shown here) exhibit the same pattern.

Attention is now turned to the prediction of two-dimensional shear flows. The numerical solutions have been obtained by solving simultaneously the set of partial differential equations comprising equation (28) for the four non-zero elements of $\overline{u_i u_j}$, equation (30) and the mean momentum equation. These flows are not homogeneous and, of course, diffusional flux terms must be included. The diffusional approximations adopted render the equation set parabolic. We have therefore based our numerical solution scheme on the well-known finite-difference procedure of Patankar & Spalding (1970). Except where otherwise indicated, model 1 has employed the invariant diffusion simulation (25), while model 2 adopted the simpler gradient-diffusion expression (26). A few exploratory calculations have shown, however, that, except for the asymmetric channel flow of Hanjalić & Launder (1972*a*) and near the outer edges of the free shear flows, a shift from one diffusion hypothesis to another has little effect on the stress profiles. Nearly all the differences between the predictions of models 1 and 2 can thus be attributed to the differences in the pressure–strain hypotheses.

A final point to make is that for these thin shear flows only the *primary* generation terms have been included in our solution of the Reynolds-stress equations, i.e. those involving $\partial U_1/\partial x_2$. We neglected terms containing $\partial U_1/\partial x_1$ in the belief that their effect was unimportant and with the knowledge that to include them would render the numerical solution scheme more cumbersome and time consuming. (Consistently the normal-stress-gradient terms in the streamwise

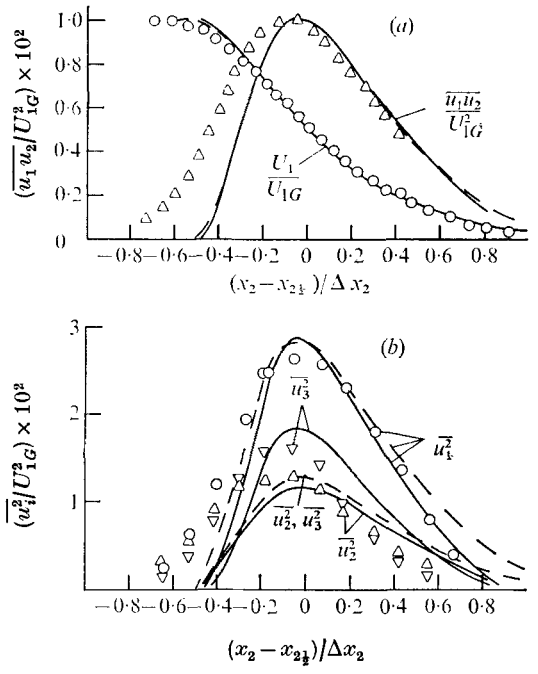

FIGURE 6. The plane mixing layer. ——, model 1; – – –, model 2. (*a*) Mean velocity and shear-stress profiles. ○, △, experiment, Bradshaw, Ferriss & Johnson (1964). (*b*) Normal-stress profiles. ○, △, ▽, experiment, Castro (1973).

mean momentum equation have also been omitted; this practice is in line with *all* thin shear flow treatments.) However Bradshaw (1973*a*) has recently drawn attention to the startlingly large influences of small secondary strain rates; in §5, therefore, the influence of these neglected terms (as implied by the present closure) is briefly examined.

Figures 6 and 7 show profiles of Reynolds stress and mean velocity in the plane mixing layer and the plane jet respectively. The mixing layer is a notoriously difficult flow to measure, there being a 50 % variation in spreading rate reported among the ten major investigations. Rodi (1972) concluded that the shear-stress and mean-velocity measurements of Bradshaw, Ferriss & Johnson (1964) displayed the best internal consistency and it is these with which comparison is made in figure 6. The mean-velocity predictions are barely distinguishable from each other and are in close agreement with the measurements except at the high velocity edge, where the predictions show a slightly faster approach to the free-stream velocity than do the measurements. The shear-stress profile shows a consistent disagreement between measurement and prediction in this region. The rate of spread of the flow is often reported in terms of $d\Delta x_2/dx_1$, Δx_2 being the lateral distance between positions where the velocity is 90 and 10 % of the free-stream velocity U_{1G}. Predictions for both models give a spreading rate of 0·16, which agrees closely with the more consistent experimental data. The normal-stress profiles are compared with the recent data of Castro (1973) in figure 6 (*b*).

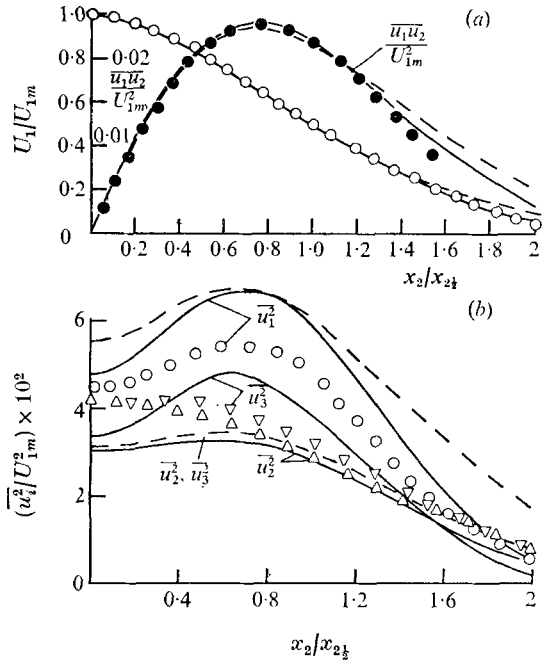

FIGURE 7. The plane jet in stagnant surroundings. ——, model 1; – – –, model 2. (*a*) Mean velocity and shear-stress profiles. ○, experiment, Robins (1971), ●, experiment, Bradbury (1965). (*b*) Normal-stress profiles. ○, △, ▽, experiment, Patel (1970).

Agreement between both sets of predictions and measurements is generally satisfactory in the central region of the shear flow though model 1 displays a somewhat larger difference between $\overline{u_2^2}$ and $\overline{u_3^2}$ than the data and model 2, of course, gives no difference at all. As with the shear-stress profile, agreement is least satisfactory near the high velocity edge.

Comparison of the predicted and measured behaviour of the plane jet in stagnant surroundings is shown in figure 7; U_{1m} denotes the streamwise velocity on the axis. Agreement of the predicted mean-velocity and shear-stress profiles with experiment is satisfactorily close;† the differences between model 1 and model 2 in the outer part of the jet are due almost entirely to the different stress diffusion hypothesis used. For both models the growth rate of the jet half-width is 0·116 compared with a mean experimental value of 0·11. The normal-stress profiles display greater departure from the measured values than was the case with the plane mixing layer, the predicted level of $\overline{u_1^2}$ being on average about 15 % too high and, as in the mixing layer, too large a separation being predicted between $\overline{u_2^2}$ and $\overline{u_3^2}$. It does not seem possible to identify with certainty the origin of these differences. To keep them in perspective, one should note that it is the stresses themselves (and not their r.m.s. values) that are plotted, and to measure r.m.s. turbulence intensity levels in free shear flows to within an accuracy of 8 % is very difficult indeed.

Figure 8 draws a comparison with the mean flow measurements of another

† Again Rodi's (1972) recommendation for the 'best' experimental data was accepted.

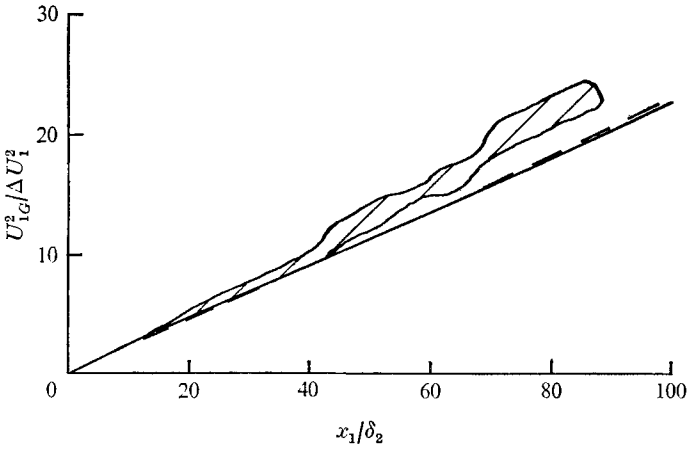

FIGURE 8. Far-field decay of plane jet in moving stream. ——, model 1; – – –, model 2; ////, envelope of data, Bradbury (1972, private communication). δ_2 = jet momentum thickness.

free shear flow, the plane jet with a shear velocity much less than that of the external stream. The figure shows the rate of decay of the centre-line velocity with distance downstream. Far enough from the jet exit this flow should attain a state of moving equilibrium where the variation of $[U_{1G}/\Delta U_1]^2$ with x_1 is linear, U_{1G} being the free-stream velocity and ΔU_1 the change in velocity from the axis to the free stream. It is not clear whether Bradbury's (1972, private communication) data ever reach this equilibrium state. The envelope of the experiments shows a slowly increasing slope as x_1 increases; conclusions at large x_1 are difficult to draw however because the width of experimental variation enlarges rapidly. Evidently the predicted behaviour exhibits a somewhat too slow rate of decay, model 1 being slightly the worse in this respect.

In this flow the relative magnitude of the terms in a turbulence energy balance is substantially different from that in the mixing layer or the jet in stagnant surroundings. For the latter, the ratio of average generation to dissipation rates of k across the flow is equal to or greater than unity; they may be designated 'strong' shear flows. In the asymptotic jet, however, the importance of the production term progressively diminishes with distance downstream, leading to a correspondingly large convective transport; this facet is characteristic of weak shear flows. Models of turbulence simpler than the one used here fail to predict (by a wider margin) the correct rate of spread of both the strong and weak shear flows (cf. Rodi 1972). That the Reynolds-stress closure used here, with constants adjusted to suit the strong shear flows, should also fail to predict the correct rate of spread of the weak shear flows is a little disappointing. This topic is discussed further in § 5.

The last free shear flow considered is the wake behind a thin flat plate, examined by Chevray & Kovasznay (1969). Unlike the two-dimensional shear flows considered hitherto, this is a strongly non-equilibrium flow and the initial profiles exert a significant effect on the development for some distance downstream. Computations were begun at the trailing edge of the plate, where measured values of

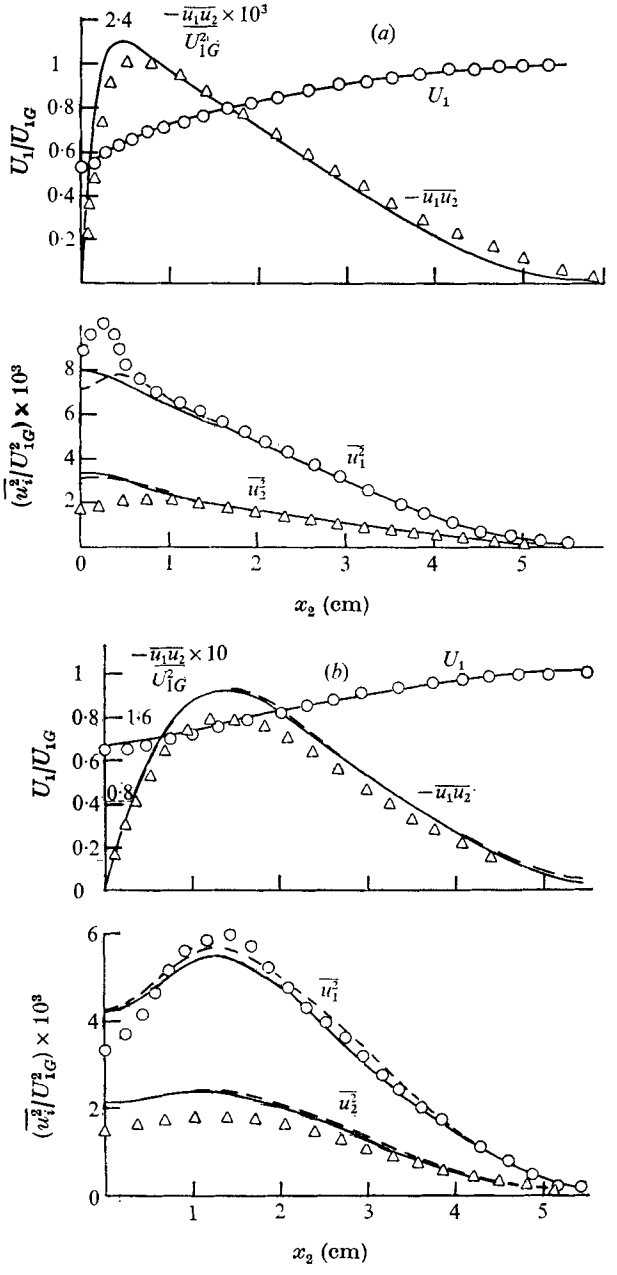

FIGURES 9(*a*, *b*). For legend see next page.

U_1, $\overline{u_1^2}$, $\overline{u_2^2}$ and $\overline{u_1u_2}$ provided the starting profiles. In the absence of data for $\overline{u_3^2}$ we adopted Klebanoff's (*1955*) measured values and then determined the profile of ϵ from the formula

$$\epsilon = 0{\cdot}3k\,\partial U_1/\partial x_2. \tag{32}$$

Equation (32) has the effect of putting the dissipation rate of turbulence energy equal to the generation rate over most of the flow since the shear stress is very

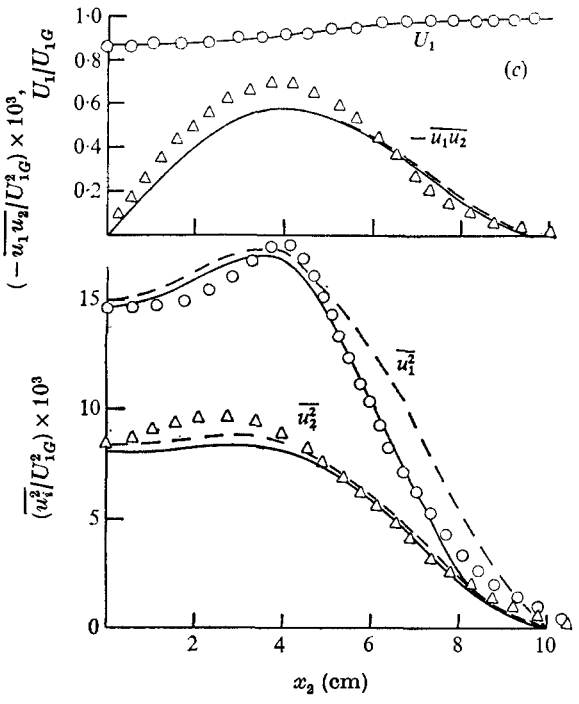

FIGURE 9. Development of wake behind flat plate; mean velocity and Reynolds-stress profiles. ——, model 1; – – –, model 2; ○, △, experiment, Chevray & Kovasznay (1969). (*a*) $x_1 = 5$ cm. (*b*) $x_1 = 20$ cm. (*c*) $x_1 = 240$ cm.

nearly equal to $-0{\cdot}3k$. Over the outer 25% of the boundary layer, however, (32) provides a somewhat better estimate of ϵ than would be obtained by equating the generation and dissipation rates of turbulence energy.

Profiles of mean velocity and Reynolds stress are compared with experiment at 0·05 m, 0·2 m and 2·4 m behind the plate in figure 9. Generally there is very close correspondence between the predicted and measured profiles. Indeed, for the normal stresses, agreement is much better than for the cases of the mixing layer or the plane jet shown in figures 6 and 7 (a result which makes one regret that measurements of $\overline{u_3^2}$ were not made). However at the first two stations the normal-stress profiles near the axis are not well predicted, $\overline{u_2^2}$ being too large and $\overline{u_1^2}$ too small. We think that the discrepancy here is probably attributable to a residual near-wall influence on the pressure–strain correlation immediately behind the plate.

Attention is now turned to the prediction of flow in a plane channel. In this case the finite-difference solutions used the boundary conditions given in table 3 applied in the fully turbulent region close to the walls. The following points should be noted: the well-known semilogarithmic law provides the basis for fixing the mean velocity; the boundary condition on $\overline{u_1u_2}$ is given by the mean momentum equation (dP/dx denoting the gradient of static pressure along the duct); the coefficients in the normal-stress boundary conditions represent a consensus of several of the most thoroughly documented wall flows; and finally,

Quantity	Near-wall value
U_1	$\begin{cases}(U_\tau/0{\cdot}42)\ln x_2^+ + 5{\cdot}45 & \text{(smooth)} \\ (U_\tau/0{\cdot}42)\ln x_2/e + 3{\cdot}5 & \text{(rough)}\dagger\end{cases}$
$\overline{u_1u_2}$	$-U_\tau^2 + x_2 dP/dx_1$
$\overline{u_1^2}$	$5{\cdot}1U_\tau^2$
$\overline{u_2^2}$	$1{\cdot}0U_\tau^2$
$\overline{u_3^2}$	$2{\cdot}3U_\tau^2$
ϵ	$-\overline{u_1u_2}\, dU_1/dx_2$

† e is the height of the roughness elements.

TABLE 3. Near-wall boundary conditions for channel flow

the boundary condition on ϵ follows directly from the neglect of diffusion in the transport equation for turbulence energy.

The distributions of mean velocity and Reynolds normal stresses for the symmetric channel are shown in figure 10. The mean velocity profile for model 1 falls within the envelope of Laufer's (1951) and Hanjalić's (1970) data at comparable Reynolds numbers; that for model 2 is a somewhat fuller profile. Predicted turbulence-intensity profiles are shown in figure 10 (*b*) and compared with the data of Comte-Bellot (1965). Agreement is generally satisfactory though it is noted that model 2 gives too small a separation of $\overline{u_2^2}$ and $\overline{u_3^2}$ (that it should give *any* separation is mainly due to the effects of the near-wall correction (24) to the pressure–strain term).

A more searching test is the asymmetric channel flow of Hanjalić & Launder (1972*a*). In this experiment one of the channel walls was roughened, causing a shear-stress ratio of about 5 : 1 between the walls. Figure 11 (*a*) shows the predicted profiles of mean velocity and shear stress across the channel, the rough wall being on the left. The measured shear stress (deduced from the static pressure gradient and a Preston-tube measurement of the smooth-wall stress) and the model 1 predictions are indistinguishable from each other. For model 2 the position of zero shear stress lies a little too close to the smooth surface. Agreement is not quite so good for the mean velocity; for model 1 of the pressure–strain approximation the predicted velocity profile is a little fuller than that measured in the mid-channel region. For model 2, the mean velocity profile is rather unsatisfactory.

As remarked above, the diffusion terms in the stress equation have a strong influence on this flow. This fact is well brought out in figure 12, which shows the turbulence-intensity profiles for the two diffusion approximations and the two pressure–strain hypotheses. The code letters *a* and *b* refer to the diffusion approximations (25) and (26) respectively (thus models 1 (*a*) and 2 (*b*) are precisely the same as those designated models 1 and 2 on earlier figures). With model 1 (*a*) the profiles of u_1 and u_2 are predicted reasonably well but the level of u_3 falls slightly below the measured value in the vicinity of the maximum mean velocity. When, instead, the simple diffusion hypothesis is employed (model 1 *b*) then the u_2 profile is improved, and the u_3 profile lies much closer to the experimental values. Overall, the simple diffusion hypothesis [equation (26)] gives slightly

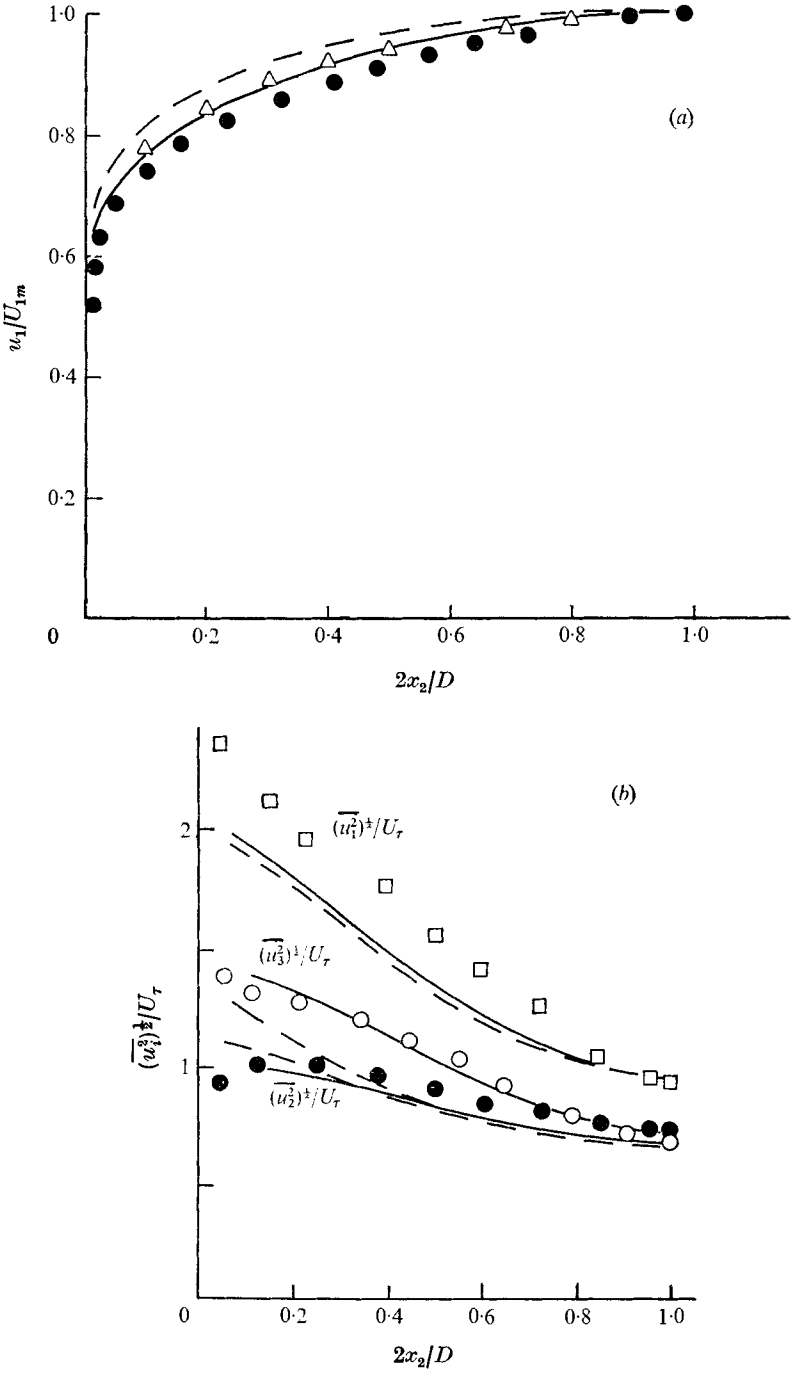

FIGURE 10. Fully developed symmetric channel flow. ——, model 1; – – –, model 2. (*a*) Mean velocity profiles. △, experiment, Laufer (1951); ●, experiment, Hanjalić (1970). (*b*) Turbulence intensity distributions. □, ○, ●, experiment, Comte-Bellot (1965).

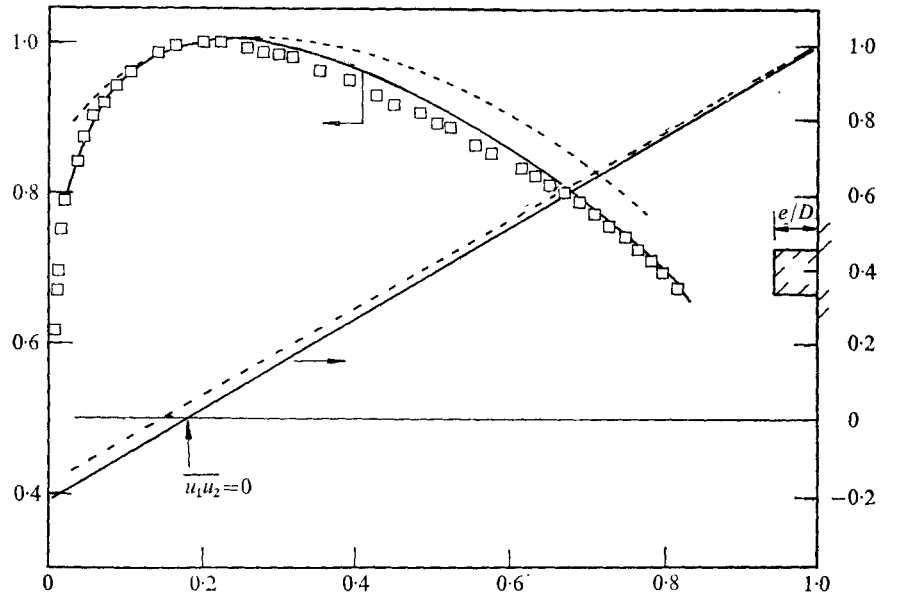

FIGURE 11. Fully developed asymmetric channel flow: mean velocity and shear stress. ——, model 1; – – – –, model 2; □, experiment, Haujalić & Launder (1972*a*).

better agreement than the invariant form. In particular the 3:1 ratio in the effective diffusion coefficient for u_2 and u_3 implied by (25) is not borne out by experiment.† The above conclusion is reinforced by the predictions with the simpler pressure–strain hypothesis. Version 2 (*b*) gives distinctly better predictions than does 2 (*a*); the latter gives u_3 less than u_2 over about 50 % of the channel because there is insufficient diffusional transport of u_3. These model 2 predictions are inferior to the corresponding model 1 profiles.

The final test case considered is the high-Reynolds-number flat-plate boundary layer. The flow is rather similar to the symmetric channel flow and the level of agreement displayed by models 1 and 2 in figure 13 is what one would expect in view of the results shown in figure 10. The predicted wall shear stresses for models 1 and 2 are respectively 5 and 15 % higher than Klebanoff's measurements; this is consistent with the mean velocity profiles shown in figure 13 (*a*). Perhaps the most interesting question is whether the linear form for $f(l/x_2)$ adopted in (24) would give a sufficiently fast decay of the near-wall effect away from the vicinity of the surface. The indications are that it *does* seem to. Indeed the pronounced inflexion in the predicted profiles of $(\overline{u_1^2})^{\frac{1}{2}}/U_\tau$ midway across the boundary layer (which closely matches the measured behaviour) is due to a fairly rapid decrease in the wall effect in this region.

5. Concluding remarks

At the start of the numerical study of turbulent flows reported above, it was felt that the main obstacle to a satisfactory Reynolds-stress closure for high-

† Use of (25), however, does give better predictions of the normal stresses near the edge of free shear flows.

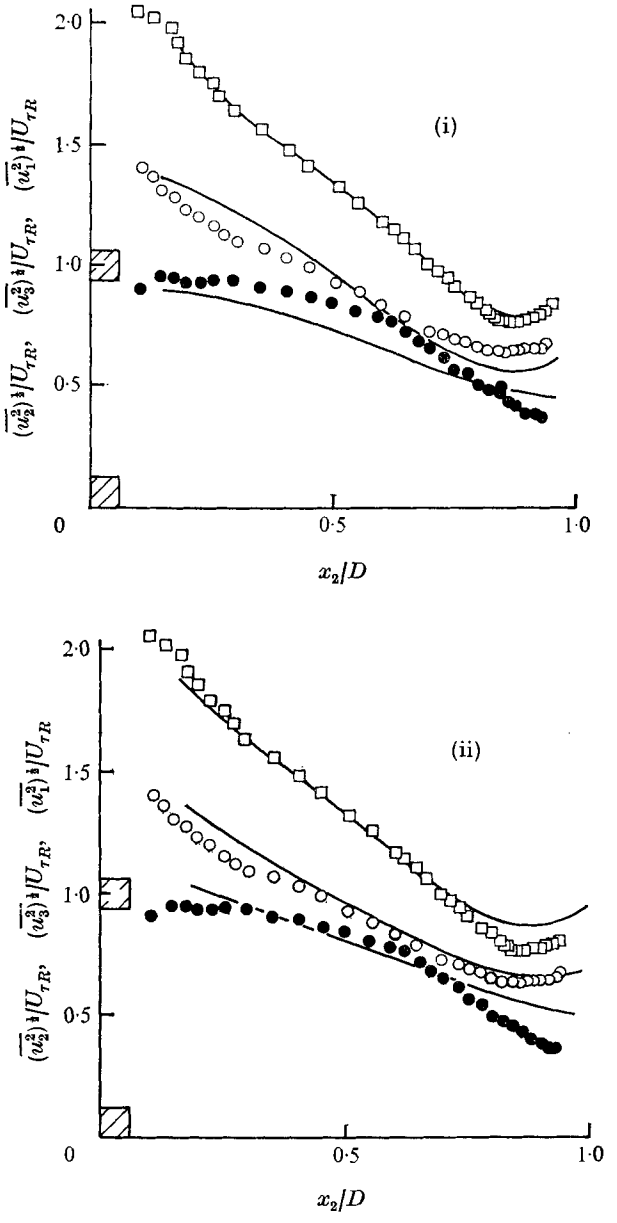

FIGURES 12 (i, ii). For legend see next page.

Reynolds-number turbulence lay in the modelling of the pressure–strain terms. We no longer believe this to be the case. For while the numerical solutions are not in perfect agreement with experimental data, few of the discrepancies can be attributed with certainty to shortcomings in the pressure–strain approximations. Inaccuracies in representing the dissipation or diffusion processes or, indeed, in the measured turbulence quantities often seem to provide a more probable source of disagreement. Both the pressure–strain hypotheses led to broadly the correct

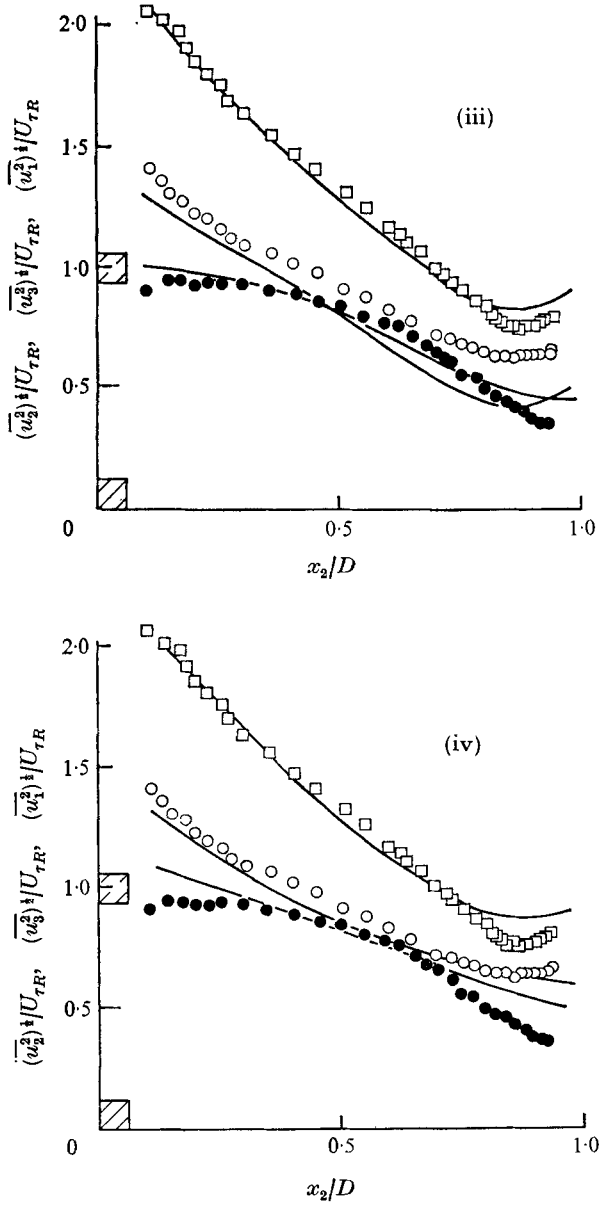

FIGURE 12. Turbulence intensity profiles in asymmetric channel flow. (i) Model 1(*a*). (ii) Model 1(*b*). (iii) Model 2(*a*). (iv) Model 2(*b*).

development of the turbulent and mean flow fields over a fairly wide range of conditions. Better overall agreement was obtained with model 1. While model 2 achieved virtually as satisfactory results in the free shear flows (including the homogeneous shear layer) it performed less well than model 1 in the different strain fields provided in Uberoi's (1956) axisymmetric contraction and Tucker & Reynolds' (1968) plane-strain experiments. (Model 2 gave worse accuracy in the

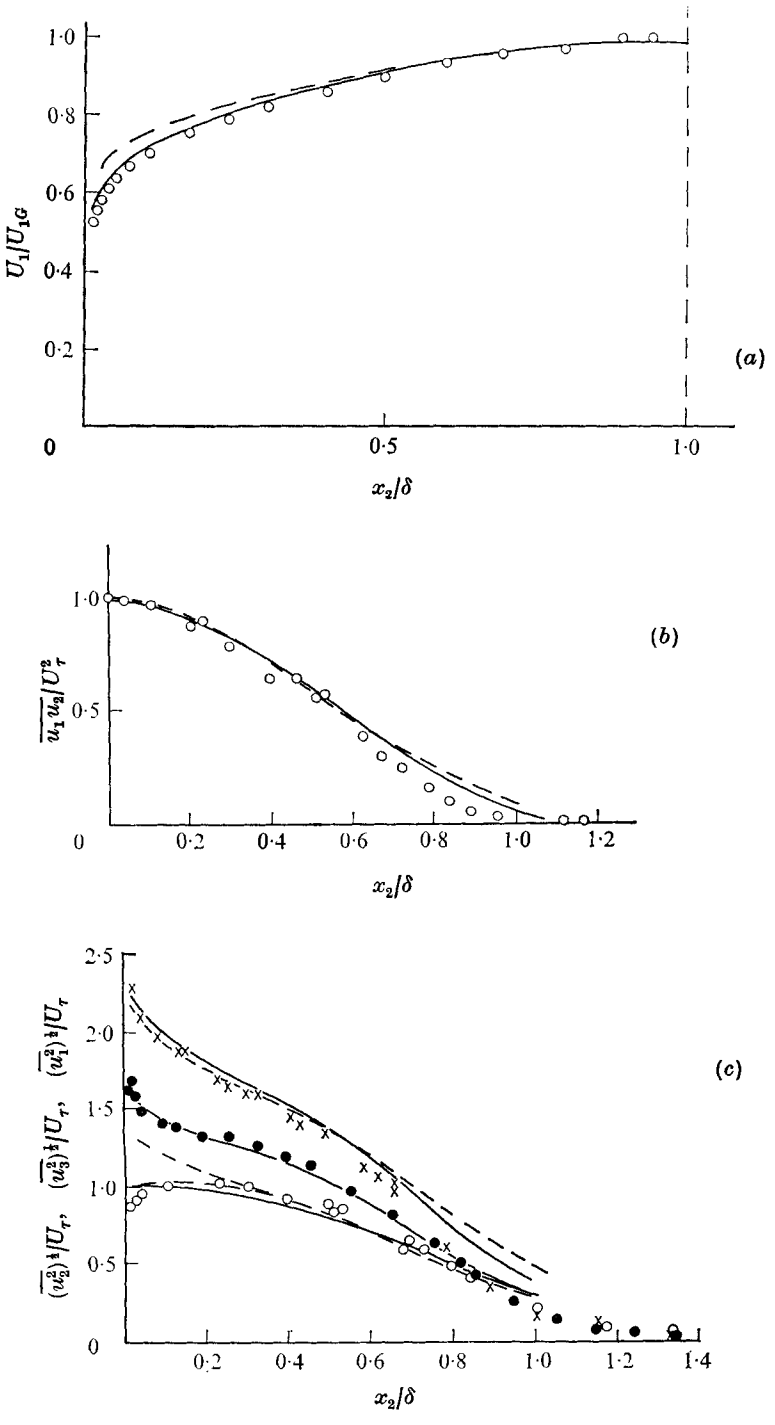

FIGURE 13. Flat-plate boundary layer. ——, model 1; – – –, model 2; ○, ●, ×, experiment, Klebanoff (1955). (*a*) Mean velocity profiles. (*b*) Shear-stress profiles. (*c*) Turbulence intensity profiles.

wall flows too though this was partly because the coefficients in the near-wall correction were chosen to suit model 1.)

Since, with model 1, the effect of mean strain on the pressure–strain term has been largely determined by general kinematic constraints, there seems reason to hope that the approximated form will give the correct trends in more complicated strain fields than those considered here. An important example of a more complicated strain field is that due to flow over curved surfaces. In this case it may easily be shown that the present pressure–strain model does imply approximately the correct effect. Bradshaw (1973*a*) has commented that prediction of these flows correctly requires the coefficient of the secondary strain term $\partial U_2/\partial x_1$ in the shear-stress equation to be an order of magnitude larger than the coefficient of the primary strain $\partial U_1/\partial x_2$. (A simple eddy-viscosity approach to curved flows would imply that the coefficients of the primary and secondary strain terms were equal.) Now, for near-wall turbulence, the present proposals give the following mean-strain terms in the shear-stress equation:

$$\left.\begin{aligned} &-1{\cdot}0\,[\overline{u_2^2}\,\partial U_1/\partial x_2+\overline{u_1^2}\,\partial U_2/\partial x_1], && \text{true generation;}\\ &+0{\cdot}70\,(\overline{u_2^2}\,\partial U_1/\partial x_2+\overline{u_1^2}\,\partial U_2/\partial x_1),\\ &-0{\cdot}18k(\partial U_1/\partial x_2+\partial U_2/\partial x_1),\\ &+0{\cdot}17(\overline{u_1^2}\,\partial U_1/\partial x_2+\overline{u_2^2}\,\partial U_2/\partial x_1), \end{aligned}\right\} \quad \text{pressure–strain effects.}$$

On collecting terms and inserting the values $\overline{u_1^2} = 1{\cdot}1k$ and $\overline{u_2^2} = 0{\cdot}25k$, which are typical for the near-wall region, the mean-strain terms may be expressed as

$$0{\cdot}06k\frac{\partial U_1}{\partial x_2}\left(1+8\frac{\partial U_2/\partial x_1}{\partial U_1/\partial x_2}\right),$$

i.e. an 8-fold amplification of the secondary strain effect.

Bradshaw also attributes the difficulty of predicting both strong and weak free shear flows with a single set of coefficients to the influence of the secondary strain terms $\partial U_1/\partial x_1$ and $\partial U_2/\partial x_2$. These terms are only about one and a half orders of magnitude smaller than $\partial U_1/\partial x_2$ in the mixing layer and plane jet in stagnant surroundings but are entirely negligible in the axisymmetric jet or wake. Here it must be said that, according to the present pressure–strain hypotheses, *these terms do not enter the shear-stress equation*. They *do* appear in the normal-stress equations and hence (since the normal stresses appear in the shear-stress equation) they indirectly affect the level of shear stress. It appears unlikely however that this connexion will be strong enough for the secondary strain terms to exert much effect.

There is of course the distinct possibility that the current pressure–strain approximations do not contain some important effect. We believe, however, that the simulated form of the equation for the energy dissipation rate (particularly regarding the influence of mean strain on the level of ϵ) provides an equally probable source of the strong/weak shear-flow paradox. Indeed we tend to view a thorough reappraisal of that equation and an assessment of the validity of the assumption of local isotropy as the most urgent research tasks in extending further the range of applicability of the present model.

We gratefully acknowledge the support provided for this research by the Science Research Council through grant B/RG/1863, by the Berkeley Nuclear Laboratories of the CEGB and by the Central Electricity Research Laboratories, Leatherhead. Our thanks are due also to Mr P. Bradshaw and Dr D. Naot for reading and providing helpful comments on an earlier version of the manuscript.

REFERENCES

BATCHELOR, G. K. & PROUDMAN, I. 1954 The effect of rapid distortion of a fluid in turbulent motion. *Quart. J. Mech. Appl. Math.* **7**, 83.

BATCHELOR, G. K. & TOWNSEND, A. A. 1948 Decay of isotrophic turbulence in the initial period. *Proc. Roy. Soc.* A **193**, 539.

BRADBURY, L. J. S. 1965 The structure of a self-preserving turbulent plane jet. *J. Fluid Mech.* **23**, 31.

BRADSHAW, P. 1972 The understanding and prediction of turbulent flow. *Aero. J.* **76**, 403.

BRADSHAW, P. 1973*a* Effects of streamline curvature on turbulent flow. *AGARDograph*, no. 169.

BRADSHAW, P. 1973*b* The strategy of calculation methods for complex turbulent flows. *Imperial College Aero. Rep.* no. 73-05.

BRADSHAW, P., FERRISS, D. H. & JOHNSON, R. F. 1964 Turbulence in the noise-producing region of a circular jet. *J. Fluid Mech.* **19**, 591.

CASTRO, I. 1973 A highly distorted free shear layer. Ph.D. thesis, University of London.

CHAMPAGNE, F. H., HARRIS, V. G. & CORRSIN, S. 1970 Experiments on nearly homogeneous shear flow. *J. Fluid Mech.* **41**, 81.

CHEVRAY, R. & KOVASZNAY, L. S. G. 1969 Turbulence measurements in the wake of a thin flat plate. *A.I.A.A. J.* **7**, 1641.

CHOU, P. Y. 1945 On velocity correlations and the solutions of the equations of turbulent fluctuation. *Quart. Appl. Math.* **3**, 38.

COMTE-BELLOT, G. 1965 Ecoulement turbulent entre deux parois parallèles. *Publ. Sci. Tech. Ministère de l'Air*, no. 419.

CROW, S. C. 1968 Viscoelastic properties of fine-grained incompressible turbulence. *J. Fluid Mech.* **41**, 81.

DALY, B. J. & HARLOW, F. H. 1970 Transport equations of turbulence. *Phys. Fluids*, **13**, 2634.

DONALDSON, C. DUP. 1968 A computer study of an analytical model of boundary layer transition. *A.I.A.A. Paper*, no. 68–38.

DONALDSON, C. DUP. 1971 A progress report on an attempt to construct an invariant model of turbulent shear flows. *Proc. AGARD Conf. on Turbulent Shear Flows, London*, paper B-1.

HANJALIĆ, K. 1970 Two-dimensional flow in an axisymmetric channel. Ph.D. thesis, University of London.

HANJALIĆ, K. & LAUNDER, B. E. 1972*a* Asymmetric flow in a plane channel. *J. Fluid Mech.* **51**, 301.

HANJALIĆ, K. & LAUNDER, B. E. 1972*b* A Reynolds stress model of turbulence and its application to thin shear flows. *J. Fluid Mech.* **52**, 609.

IRWIN, H. P. A. 1973 Measurements in a self-preserving plane wall jet in a positive pressure gradient. *J. Fluid Mech.* **61**, 33.

KLEBANOFF, P. S. 1955 Characteristics of turbulence in a boundary layer with zero pressure gradient. *N.A.C.A. Rep.* no. 1247.

LAUFER, J. 1951 Investigation of turbulent flow in a two-dimensional channel. *N.A.C.A. Rep.* no. 1053.

LUMLEY, J. L. 1972 A model for computation of stratified turbulent flows. *Int. Symp. on Stratified Flow, Novisibirsk.*

LUMLEY, J. L. & KHAJEH-NOURI, B. 1974 Computational modelling of turbulent transport. *Proc. 2nd IUGG–IUTAM Symp. on Atmos. Diffusion in Environmental Pollution*, Academic.

NAOT, D., SHAVIT, A. & WOLFSHTEIN, M. 1970 Interactions between components of the turbulent velocity correlation tensor. *Israel J. Tech.* **8**, 259.

NAOT, D., SHAVIT, A. & WOLFSHTEIN, M. 1972 Prediction of flow in square section ducts. *Mech. Engng Dept., Technion, Haifa, Intern. Rep.* no. 154.

NAOT, D., SHAVIT, A. & WOLFSHTEIN, M. 1973 Two-point correlation model and the redistribution of Reynolds stress. *Phys. Fluids*, **16**, 738.

PATANKAR, S. V. & SPALDING, D. B. 1970 *Heat and Mass Transfer on Boundary Layers.* London: Intertext Books.

PATANKAR, S. V. & SPALDING, D. B. 1972 A calculation procedure for heat, mass and momentum transfer in three-dimensional parabolic flows. *Int. J. Heat Mass Transfer*, **15**, 1787.

PATEL, R. P. 1970 A study of two-dimensional symmetric and asymmetric turbulent shear flows. Ph.D. thesis, McGill University.

REYNOLDS, W. C. 1970 Computation of turbulent flows–state-of-the-art, 1970. *Stanford University Mech. Engng Dept. Rep.* MD-27.

ROBINS, A. 1971 The structure and development of a plane turbulent free jet. Ph.D. thesis, University of London.

RODI, W. 1972 The prediction of free turbulent boundary layers by use of a 2-equation model of turbulence. Ph.D. thesis, University of London.

ROTTA, J. C. 1951 Statistische Theorie nichthomogener Turbulenz. *Z. Phys.* **129**, 547.

ROTTA, J. C. 1962 Turbulent boundary layers in incompressible flow. *Prog. Aero. Sci.* **2**, 1.

TENNEKES, H. & LUMLEY, J. L. 1972 *A First Course in Turbulence.* M.I.T. Press.

TOWNSEND, A. A. 1954 The uniform distortion of homogeneous turbulence. *Quart. J. Mech. Appl. Math.* **7**, 104.

TUCKER, H. J. 1970 The distortion of turbulence by irrotational strain. *McGill University, Mech. Engng Dept. Rep.* no. 70-7.

TUCKER, H. J. & REYNOLDS, A. J. 1968 The distortion of turbulence by irrotational plane strain. *J. Fluid Mech.* **32**, 657.

UBEROI, M. S. 1956 Effect of wind-tunnel contraction on free-stream turbulence. *J. Aerospace Sci.* **23**, 754.

UBEROI, M. S. 1957 Equipartition of energy and local isotropy in turbulent flows. *J. Appl. Phys.* **28**, 1165.

UBEROI, M. S. 1963 Energy transfer in isotropic turbulence. *Phys. Fluids*, **6**, 1048.